

# DSI Suppression with Adaptive Beamforming in DVB-T Passive Radar Measurements

Kyrre Strøm\*, Øystein Lie-Svendsen\*, Idar Norheim-Næss\*, Terje Johnsen\*, Erlend Finden\*, Karl Erik Olsen\*

\*Norwegian Defence Research Establishment (FFI)

P.O. Box 25, NO-2027 Kjeller, Norway

email: {Kyrre.Strom, Oystein.Lie-Svendsen, Idar.Norheim-Nass, Terje.Johnsen, Erlend.Finden, Karl-Erik.Olsen}@ffi.no

**Abstract:** Adaptive beamforming (ABF) for maximizing the signal to interference plus noise ratio (SINR) is applied to acquisitions made by a passive bistatic radar (PBR) exposed to strong direct signal interference (DSI). The DVB-T transmitter was located approximately  $20^\circ$  from boresight. ABF is applied after the formation of range Doppler maps where the formation was based on reconstruction of the reference signal and reciprocal filtering. Acquisition was done both with a linear array antenna of 11 horizontally polarized bowtie elements, and with two co-located linear arrays of 5 bowtie elements each, one horizontally polarized and the other vertically polarized. A small GPS equipped aircraft was used as target. The aircraft GPS data was used to find the bistatic range and Doppler, and the SINR was measured at this target location for half an hour. The Distortionless (DL) ABF obtains notably improved SINR compared to the conventional beamformer for the antennas co-polarized with the transmitter, on average 4.5dB for 11-elements and 2dB for 5-elements. Less than 1 dB improvement was achieved for the 5-element cross-polarized antenna. Stationary interference allowed for defining the DL beamformer by the same spatial covariance matrix with no updates throughout an acquisition of half an hour without deteriorating the beamformer response notably.

## 1. Introduction

Passive bistatic radars (PBR) are dependent on external illuminators of opportunity. The PBR location needs to be illuminated by the transmitter, and direct signal interference (DSI) and terrain scattering interference is an ever-recurring problem for PBR. Using an antenna that is cross-polarized with the transmitter is an option to mitigate the DSI and was considered in [10]. The benefit from DSI suppression offered by the cross-polarized antenna did not, in those observations, overcome the disadvantage of seemingly lower cross-polarized target RCS. Several signal processing techniques have been investigated for mitigating DSI and clutter suppression, including direct signal cancellation [1]. A technique for DSI suppression in digital video broadcasting (DVB) and audio broadcasting is mismatched filtering of surveillance signal with the reconstructed reference signal, denoted reciprocal filtering [9].

Array processing may form antenna receiver beams with nulls in direction of the transmitter [3]. One study [5] applied adaptive beamforming with a Metropolitan Beacon System based PBR for mitigating elevation related interference, and thereafter time-based DSI suppression.

In this paper we utilize adaptive beamforming in a DVB-T based PBR system. ABF is applied after the range Doppler processing that has made use of reciprocal filtering for DSI suppression. Using ABF we do not need to know the exact location of the signal source as would be the case for explicit nulling. Multipath of transmitted signals will also broaden the interfering signals angle of arrival for the PBR, which is hard to counteract by explicit nulling. We apply the Distortionless (DL) beamformer, a spatial filter maximizing the signal to interference plus noise ratio [7]. Sample matrix inversion [6] is used to estimate the noise plus interference spatial covariance matrix for the array. The target SINR obtained by the distortionless and the conventional beamformer is compared at a fairly large set of consecutive CPIs ( $> 10^3$ ) for each of the acquisitions conducted. From the aircraft GPS information the target range Doppler location is easily found.

The PBR system applied during measurements is developed at Fraunhofer FHR [8], with exception of the receiver antenna which is developed at the Norwegian Defence Research Establishment [2].

## 2. Acquisition of data

The experiment and equipment is described in detail elsewhere [10], and we recapture it briefly here for convenience. The PBR antenna is a reconfigurable horizontally oriented linear array consisting of 11 crossed bowtie elements. The first measurement made acquisitions with 11 H-pol bowtie elements. Two days later the second acquisition was conducted with 5 H-pol and 5 V-pol bowtie elements, making two orthogonally polarized uniform linear arrays of 5 elements each with identical location. Properties of the antenna is described in [2]. One of the array elements was used for acquiring the reference signal from the transmitter. The horizontally polarized DVB-T transmitter at Halden was located 74km from the PBR, with 63kw effective isotropic radiated power, and at  $20^\circ$ - $25^\circ$  from antenna boresight. Hence the antenna was exposed to strong direct signal interference. A small GPS equipped aircraft, Cessna 172m, served as a cooperating target during the experiment following prescribed trajectories. Fig. 1 left panels shows the trajectory flown during the first acquisition and the right panel during the second acquisition.

## 3. Signal processing and beamforming

The PBR software reconstructs the reference signal according to the DVBT-standard, and performs range compression by a mismatched filtering of the surveillance signal with the reference signal, reciprocal filtering. Although this filtering suppresses DSI well [9], some interference remains after filtering.

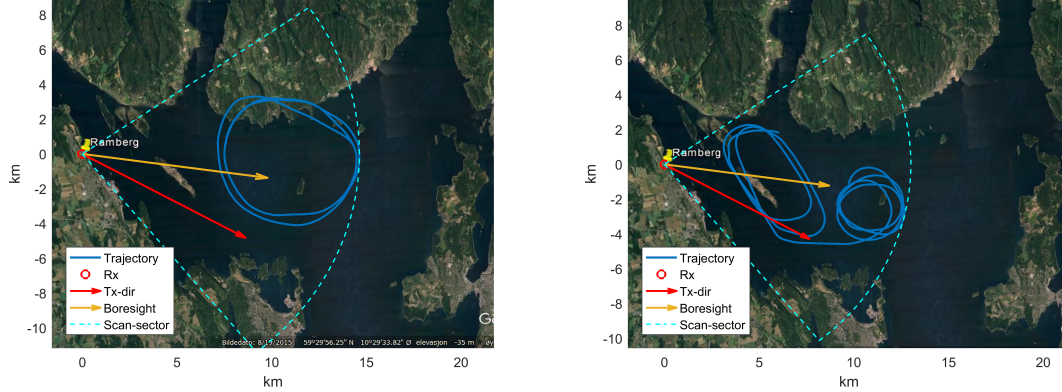


Figure 1: Aircraft trajectories in the two acquisitions. The receiving PBR antenna is indicated with a yellow thumbtack, the antenna boresight is shown with a yellow arrow and the direction towards the Halden DVBT-transmitter is indicated with a red arrow. Left plot shows acquisition with 11 element H-pol array and with  $2 \times 5$  element H-pol and V-pol to the right.

The PBR has one receiver channel for each antenna element, and stacking the range Doppler maps produced for each channel on top of each other, we picture a data cube. Each horizontal layer in the cube is the range Doppler map of the corresponding antenna element. A column in the data cube through the same range Doppler cell of all the channels will be denoted a range Doppler array snapshot, or simply a snapshot. The spatial filter constituting the beamformer is defined by a set of complex weights  $\mathbf{w} = [w_1, \dots, w_n]^t$ , where  $n$  is the number of channels in the array. The beamformer response to a snapshot  $\mathbf{y} = [y_1, \dots, y_n]^t$  is the coherent sum  $\mathbf{w}^H \mathbf{y}$  where  $\mathbf{w}^H$  denotes the conjugate transpose of  $\mathbf{w}$ . The weights defining the DL beamformer solves the following quadratic optimization problem,

$$\min_{\mathbf{w}} \mathbf{w}^H \mathbf{K} \mathbf{w} \quad \text{subject to} \quad \mathbf{w}^H \mathbf{s} = 1 \quad (1)$$

where the solution is [11]

$$\mathbf{w} = \frac{\mathbf{K}^{-1} \mathbf{s}}{\mathbf{s}^H \mathbf{K}^{-1} \mathbf{s}} \quad (2)$$

Here  $\mathbf{K}$  is the spatial noise plus interference covariance matrix for the range Doppler column under test. The steering vector  $\mathbf{s} = \mathbf{s}(\vartheta)$ ,  $s_j = \exp(-2\pi j d / \lambda \sin(\vartheta))$  for  $j = 1, \dots, n$ , is the array response for signal arriving from azimuth angle  $\vartheta$  relative to boresight of the uniform linear array antenna. The antenna element spacing is  $d = 0.26m$ , and wavelength  $\lambda = 0.45m$  for the center frequency of the band acquired during the experiment. When  $\mathbf{s}$  is the steering vector in direction of the target,  $\mathbf{w}$  are the weights maximizing the signal to noise plus interference ratio, [7]. If the spatial covariance matrix  $\mathbf{K}$  also contains the target signal contribution, the beamformer defined by  $\mathbf{w}$  is denoted the minimum variance distortionless response (MVDR) beamformer, [4]. In our processing we estimate the noise plus interference spatial covariance matrix without including the target signal, and apply the same spatial covariance matrix for all the range Doppler columns under test. Thus, our beamformer response depends linearly on the snapshots. We estimate the covariance matrix by an average of snapshot outer products,

$\mathbf{K} \sim \tilde{\mathbf{K}} = 1/N \sum_{j=1}^N \mathbf{y}^j \mathbf{y}^{jH}$ , where the  $\mathbf{y}^j$ s are snapshots taken from  $L = 28$  far range Doppler cells in each of  $M = 50$  consecutive CPIs. In total  $N = LM$  snapshots are used for averaging over time as well as range and Doppler to estimate  $\mathbf{K}$ . Covariance matrices  $\mathbf{K}$  estimated in this manner at various time intervals during an acquisition of half an hour showed only minor differences. In this paper we investigate the behavior of the DL beamformer that is defined by one and the same covariance matrix  $\mathbf{K}$  throughout the processing of the entire acquisition, and the first 50 CPIs of the acquisition is used for defining  $\mathbf{K}$ . The conventional beamformer is defined by taking the steering vector as weights,  $\mathbf{w} = \mathbf{s}$ , and in the case where  $\mathbf{K}$  in (1) is the identity matrix, the DL beamformer reduces to the conventional beamformer.

We apply both conventional and distortionless beamforming to pick candidate detections and measure SINR and azimuth of arrival. Conventional beamscan is applied to the snapshots in a search rectangle of  $7 \times 5$  cells centered at the aircraft GPS rD-coordinate as well as to a large set ( $> 10^4$ ) of far range Doppler snapshots of the current CPI, obtaining a stack of range Doppler sub-maps, one for each squinted beam. The squared amplitude of the beamformer response to a snapshot is taken as the signal value, and the noise plus interference level for the beam is taken as the mean signal values at the far range Doppler cells. The rD-cell in the search rectangle of maximum SINR over all beams is taken as the candidate target detection. The azimuth of arrival for this candidate detection is defined by the beam producing the maximum signal for the snapshot of this candidate. Due to the strong DSI this angle tends to deviate from the angle of maximum SINR. Fig. 2 blue curves show the interference dependence on scan angle for the H-pol arrays of 11 and 5 elements and V-pol 5 elements at a typical time instance. The H-pol channels both have a distinct peak of more than 10dB in direction of the transmitter, whereas the V-pol channel varies less than 1.5dB.

Similarly, we produce a candidate detection for the DL beamformer where the weights during beamscan is defined by (1). The SINR of this candidate is given by the DL beamformer, but the angle of arrival is defined using the conventional beamformer. The covariance matrix in (1) does not include contributions from the target signal, only from the interference. So even though the DL beamformer maximizes the SINR at the target rD-cell, it is not suitable for determining the target signal angle of arrival. However, for the interference signal it is. The expectation for the squared amplitude of the DL beamformer response to the interference signal is given by the reciprocal of the denominator in (2), and denoted  $P_{mv}$  for power of the minimum variance beamformer [4]. Fig. 2 shows as a function of scan angle the approximation to  $P_{mv}$  obtained by using our estimated covariance matrix, which is constant throughout the CPIs. For CPIs near the trajectory start time the approximated  $P_{mv}$  more or less coincides with the beamscan defined interference from the DL beamformer, even though the  $P_{mv}$  estimate was defined by only  $L = 28$  different rD-snapshots averaged over 50 consecutive CPIs whereas the beamscan defined interference was an average over a far larger set of snapshots within the current CPI only. For CPIs at the end of the two acquisitions lasting 17.5 min and 30 min, respectively, the deviations between the approximated  $P_{mv}$  and the DL beamscan interference are less than 1.5dB. Being able to use the same covariance matrix without updates is a substantial saver with respect to computational resources, and can be a key factor during real time processing.

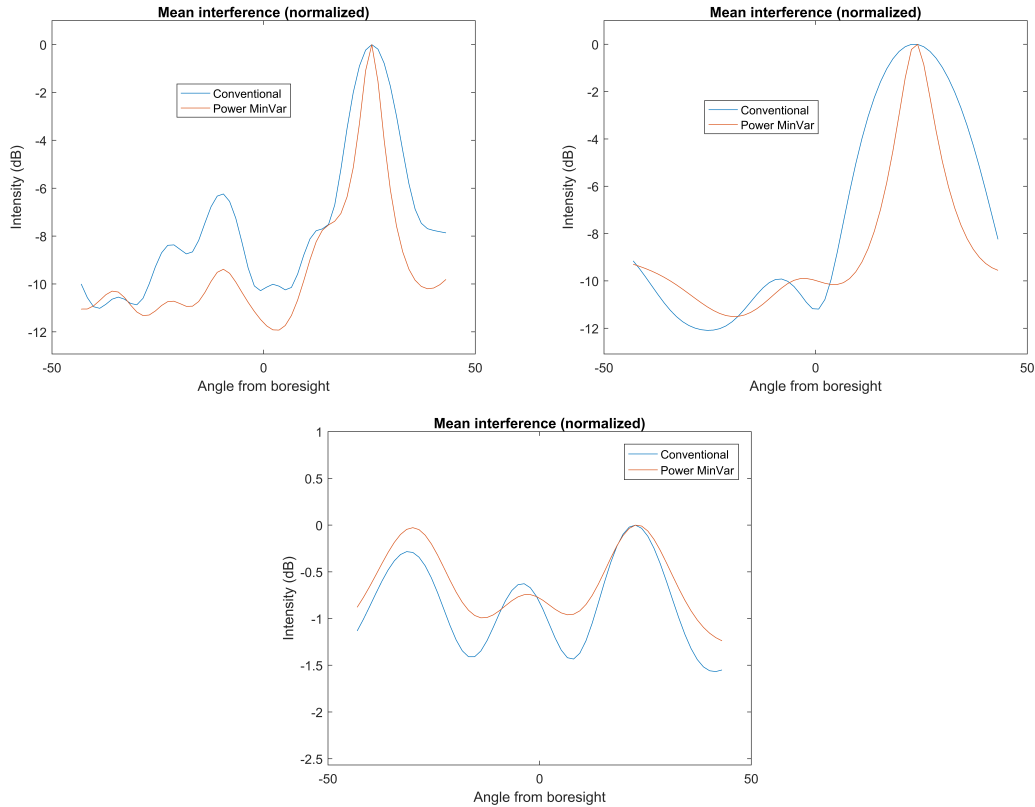


Figure 2: Normalized interference as function of scan angle for H-pol arrays with 11- and 5-elements (upper left and right) and for 5-element V-pol (lower), at typical time instances. Mean squared amplitude response at far range Doppler for conventional beamformer (blue) and the estimated  $P_{mv}$  (red) are shown, both normalized

In order to assess the behavior of the two beamformers, we need a quality criterion discriminating a valid target detection from pure noise and interference. Like in [10] we say that a candidate detection is valid provided

- The SINR should be greater than 10dB
- The bistatic Doppler should not be less than 2Hz
- The estimated azimuth direction of arrival should not deviate more than  $5^\circ$  from the direction given by the gps aircraft data.

## 4. Results

We applied the conventional and the DL beamformer to the data acquired by the 11 co-polarized antenna elements during the 17.5 min of the trajectory shown in Fig. 1. The SINR obtained during an early and late period of 100 sec are shown in Fig. 3. Only data for CPIs with valid candidates are shown, invalid candidates are replaced by straight line interpolation. The CPI was 0.5 sec and 3200 partly overlapping CPIs were processed during 17.5 min. The histogram in

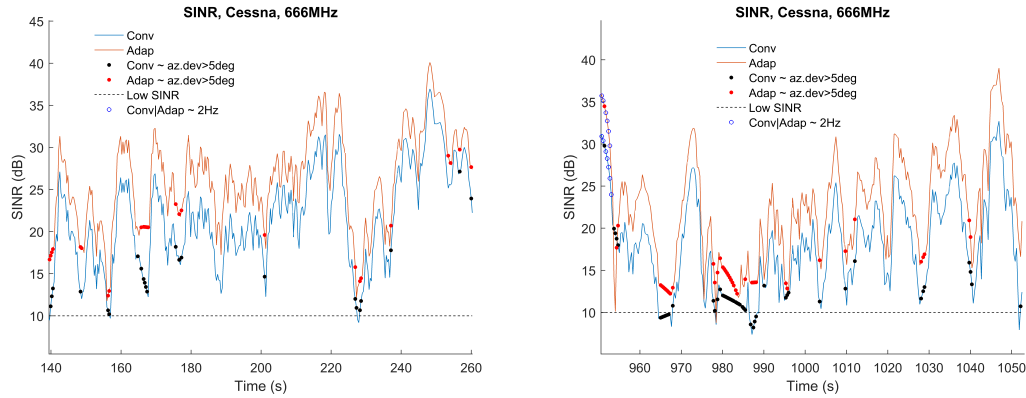


Figure 3: SINR obtained by the DL-(red) and Conventional (blue) beamformers for H-pol antenna of 11 elements during two time intervals of the first acquisition.

Fig. 4 shows the distribution of SINR improvements for the DL beamformer relative to the conventional one during the 17.5 min. The average improvement is 4.5dB. Fig. 5 shows the

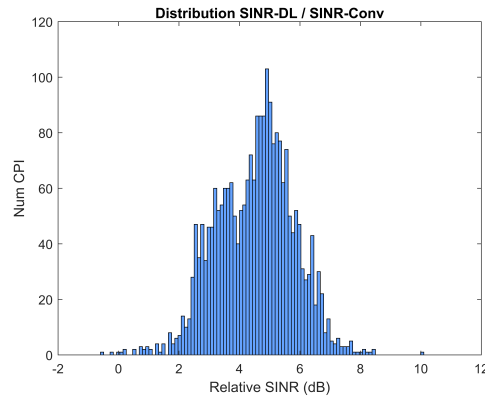


Figure 4: Distribution of SINR improvement obtained by the DL beamformer relative to the conventional one among valid candidates for the 11-elements H-pol array.

SINR obtained by the two beamformers applied to the data acquired by 5 elements array co-polarized with the transmitter during the second measurement. An early and a late time period of 200 sec during the 17.5 min long acquisition are shown. Distribution of the relative SINR improvement for the DL beamformer over the conventional one for this array is shown in Fig. 6, left panel. The average improvement is 2dB. Data from the same trajectory was also acquired by the 5 element V-polarized array, and processed by the DL and conventional beamformers. From the distribution shown in the right panel of in Fig. 6 we observe a slight improvement in SINR for the DL over the conventional one also in this case, on average 0.77dB.

The acquisitions made by the H-pol and V-pol arrays of 5-elements each were done simultaneously, making it possible to compare candidate detections from simultaneous CPIs. Previously, we found that the co- and cross-polarized antennas yielded approximately the same SINR when the conventional beamformer was applied [10]. Here we processed the same dataset using the

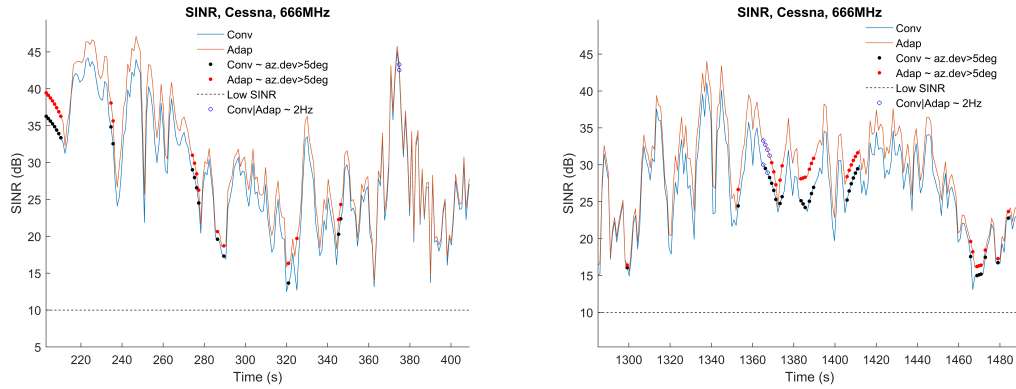


Figure 5: SINR obtained by the DL-(brown) and Conventional (blue) beamformers for H-pol antenna of 5 elements during two time intervals of the second acquisition.

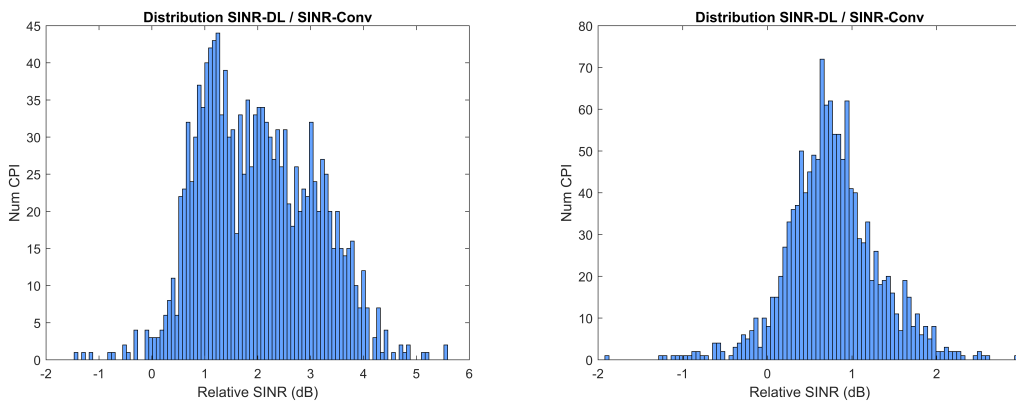


Figure 6: Distribution relative SINR of DL- and conventional beamformer for 5 element H-pol channel (left panel), and V-pol channel (right panel).

DL beamformers for the two polarization channels. In 70% of the 1740 CPIs during the 30 min acquisition both candidates were valid, and the distribution of the relative SINR ratio obtained by the H-pol and V-pol channels are shown in Fig. 7. On average, the H-pol channel has a slightly higher SINR, 1.4dB, but the distribution has a large spread and the co- and cross-pol channels seem equally advantageous also after applying the DL beamformers. It should be mentioned that in the remaining 30% of the time instances, the number of valid candidates is somewhat higher for the H-pol than the V-pol channel.

Table 1 summarizes the average improvement in SINR obtained by the DL-beamformer relative to the conventional one for the various arrays. The last row shows the improvement of the DL-beamformer for the 5-element H-pol channel relative to the V-pol channel. The listed improvements were obtained by the DL beamformers when the spatial covariance matrix was estimated using  $N = 28M$  snapshots from  $M = 50$  consecutive CPIs. We also ran the same processing for  $M = 10$  and  $M = 150$ , and no substantial difference from  $M = 50$  was observed.

The SINR comparison of the two beamformer responses shown in Fig. 3-7 are made from can-

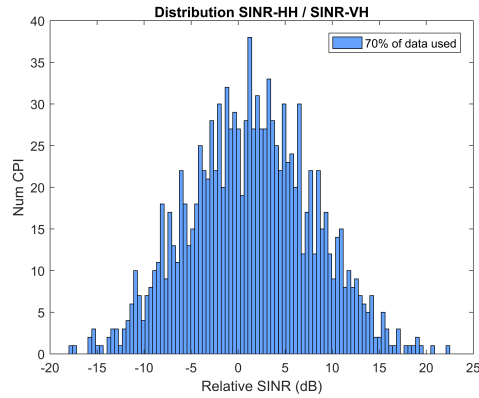


Figure 7: Distribution of SINR improvement obtained by the DL beamformer of 5-elements H-pol channel relative to the 5-element V-pol channel among the CPIs where candidate detections for both the polarizations were simultaneously valid, 70% of the total CPIs

Table 1: Average SINR improvement for the DL beamformer relative to conventional beamformer, three first rows. Last row, average SINR improvement for DL beamformer of H-pol channel relative to V-pol channel.

Antenna	Beamformers	Num CPI	Percent OK	Avg relative SINR (dB)
11H-pol	DL/conv	3203	73	4.5
5H-pol	DL/conv	1740	81	2.0
5V-pol	DL/conv	1740	76	0.77
5H-pol/5V-pol	DL	1740	70	1.4

candidate detections valid according to the three criterias listed at the end of Section 3. When producing these figures the GPS target information was used twice for every CPI and each of the beamformers. First, when picking the candidate of highest SINR, the beamscan and SINR calculations were limited to a set of snapshots in a range Doppler search rectangle. Later it was used by the angle criterion to assess the validity of the selected candidate. In a realistic detection problem knowledge about target location would not be available. To get a hint about the detection capabilities of the two beamformers from our measurements, we can compare the number of candidates fulfilling at least the SINR and Doppler criteria and compare with those fulfilling the angle criterion as well. We ran the comparison test two times for the acquisitions made by the 11H-pol element antenna, first time with the acceptance thresholds for low SINR 10dB and Doppler 2Hz as were used when producing Fig. 4. The second time the thresholds were raised to 12dB and 3Hz. Table 2 shows that the adaptive beamformer produces more valid candidates than the conventional one for both sets of thresholds, but the number of candidates discarded by the angle criterion is notably higher for the adaptive beamformer. The percentage made invalid by the angle criterion is quite sensitive to the low Doppler threshold. Care should be taken when interpreting Table 2 and when drawing conclusions about the beamformers detection capabilities from their relative SINR obtained in Fig. 3-7. In a realistic detection problem formulation the beamformer response is typically put into a likelihood ratio test derived from a statistical model of the signals, and the detection threshold would be based on an acceptable probability of false alarm ( $P_{FA}$ ). Also, sophisticated methods treating clutter regions close to the zero Doppler line



Table 2: Percentage candidate detections from DL- and conventional beamformers satisfying at least the SINR and Doppler criteria, and the percentage satisfying all three criteria. Acquisitions by 11H-pol antenna

Beamformers	Criteria and Percent OK			
	SINR > 10dB Dopp > 2Hz	SINR > 10dB Dopp > 2Hz Azm-dev < 5°	SINR > 12dB Dopp > 3Hz	SINR > 12dB Dopp > 3Hz Azm-dev < 5°
DL	90	77	82	74
Conv	83	75	72	69
Both		73		67

is often applied.

## 5. Conclusion

Adaptive beamforming was applied in a DVB-T PBR system after the formation of range Doppler maps for each channel. Data had been acquired during two measurements with a cooperating GPS-equipped small target aircraft, and the acquisitions were conducted on two different days with the DVB-T transmitter located about 20° from boresight. The first measurement was done with an antenna of 11 elements co-polarized with the transmitter. In the other two co-located array-antennas with 5 elements each were used, one co-polarized and the other cross-polarized with the transmitter. Some of the DSI for the co-polarized channels had not been removed by the mismatched filtering during the range Doppler processing, and the interference level still appeared with a distinct angular dependence. The DL beamformer applied thereafter achieved notable SINR improvement over the conventional one in the co-polarized case, about 4.5dB and 2dB on average for the 11 and 5 elements arrays respectively. Only minor improvements, less than 1 dB, were observed for the 5 elements cross-polarized channel. The noise plus interference covariance was estimated once at the beginning of each of the two acquisitions, and notable deterioration in the DL beamformer response was not observed during the two measurements of 30 min and 17.5 min. This is advantageous for real time processing, since frequent update of the spatial covariance matrix with inversion is computationally heavy and can be a limiting factor. Actual detection performance, with prescribed  $P_{FA}$ , still remains to be investigated.

## References

- [1] Cardinali, R, Colone, F, Ferretti, C & Lombardo, P 2007, Comparison of clutter and multipath cancellation techniques for passive radar. in *IEEE National Radar Conference - Proceedings.*, 4250356, pp. 469-474, *IEEE 2007 Radar Conference*, Waltham, MA, United States, 17-20 April.
- [2] E. Finden, K. Strøm, I. Norheim-Næss, M. Tømmer, Ø. Lie-Svendsen, F. Gulbrandsen and K. E. Olsen. "A Dual Polarized Crossed Bowtie Array Antenna for DVB-T Based Passive Radar." in

- Proc. 2016 IEEE International Conference on Antenna Measurements & Applications (CAMA)*, pp. 1-4, Syracuse, NY, 2016.
- [3] H. D. Griffiths, and N. R. W. Long, "Television-based bistatic radar", *IEE Proc. F: Commun. Radar and Signal Process.*, vol. 133, pp. 649–657, Dec. 1986.
- [4] D.H. Johnson, D.E. Dudgeon *Array Signal Processing: Concepts and Techniques*, Prentice Hall, Upper Saddle River, NJ, 1993, ISBN 0-13-048513-6
- [5] V. Navratil, A. O'Brian, J.L. Garry, G.E. Smith "Demonstration of Space-Time Adaptive Processing for DSI Suppression in a Passive Radar" , *Proc. 18th International Radar Symposium (IRS)*, 2017, ISSN 2155-5753, ISBN 978-3-7369-9343-3
- [6] Reed I.S, Mallett J.D, Brennan L.E , "Rapid Convergence Rate in Adaptive Arrays", *IEEE Trans. AES*, vol.10, pp. 853-861, 1974
- [7] M.A. Richards, *Fundamentals of Radar Signal Processing, 2nd Edition* McGraw-Hill Education, 2014 , ISBN 978-0-07-179832-7
- [8] J. Schell, J. Heckenbach, and H. Kuschel, "ATLANTIS, a scalable, modular PCL receiver for OFDM signals", *NATO SET-187 Specialist Meeting on Passive Radar, challenges concerning theory and practice in military application*, Szczecin, Poland, 13–14.05.2013.
- [9] S. Searle, J. Palmer, L. Davis, D. O'Hagan, and M. Ummenhofer, "Evaluation of the Ambiguity Function for Passive Radar with OFDM Transmissions", *Proc. 2014 IEEE Radar Conf.*, Cincinnati, OH, 2014, pp. 1040–1045.
- [10] K. Strøm, Ø. Lie-Svendsen, E. Finden, I. Norheim-Næss, T. Johnsen, A. Baruzzi, "DVB-T Passive Radar Dual Polarization Measurements in the Presence of Strong Direct Signal Interference", *Proc. 18th International Radar Symposium (IRS)*, 2017, ISSN 2155-5753, ISBN 978-3-7369-9343-3
- [11] H. Van Trees, *Detection, Estimation, and Modulation Theory, Optimum Array Processing, (Part IV)*, John Wiley & Sons, Inc., New-York, USA, 2002, ISBN 0-471-09390-4